

# Irradiation Induced Aging of Epoxy Resins for Impregnation of Superconducting Magnet Coils

D. M. Parragh , C. Scheuerlein , R. Piccin, F. Ravotti , *Member, IEEE*, G. Pezzullo, D. Ternova ,  
M. Taborelli , M. Lehner, and M. Eisterer 

(Invited Paper)

**Abstract**—Understanding the effect of radiation on the functional properties of epoxy resins is crucial for their application in future particle accelerators like the Future Circular Collider (FCC). We compare the irradiation induced aging rates of six epoxy resin systems that can be used for the vacuum impregnation of magnet coils. Aging is assessed based on Dynamical Mechanical Analysis (DMA), 3-point bending and outgassing tests. DMA storage and loss moduli evolutions reveal the effect of the competing influence of cross-linking and chain scission on the glass transition temperature ( $T_g$ ). The same proton and gamma irradiation dose has a similar effect on the thermomechanical epoxy resin properties. Aging rates differ strongly for the different resins, and the fastest aging is observed for the MY750 resin system, which  $T_g$  decreases with a rate of about minus 9 °C/MGy.

**Index Terms**—Accelerator magnets, DMA, epoxy resin, FCC, HL-LHC, irradiation, outgassing, short beam test.

## I. INTRODUCTION

**S**UPERCONDUCTING magnets of future particle accelerators [1] will be exposed to high radiation doses, and polymers are the magnet constituent materials most sensitive to irradiation effects. They are for instance needed for the impregnation of superconducting magnet coils [2] made of brittle conductors like Nb<sub>3</sub>Sn, to fill the porosity present after coil winding such that the mechanical stresses exerted on the coil during assembly and operation do not irreversibly degrade the conductor [3].

To qualify new polymer materials for potential use in future superconducting accelerator magnets, the CERN polymer laboratory is performing an irradiation study. The main goals of this study are to determine the effect of different radiation sources (gamma rays, protons and neutrons), different radiation atmospheres (ambient air, vacuum/inert gas) and temperatures (ambient and cryogenic temperature) on the polymer thermomechanical, thermal and dielectric properties.

In the present article we compare the effect of gamma rays, protons and neutrons at ambient temperature on the thermomechanical properties. The effect of irradiation induced aging has

Manuscript received 20 September 2023; revised 9 November 2023; accepted 9 November 2023. Date of publication 15 November 2023; date of current version 8 December 2023. (Corresponding author: C. Scheuerlein.)

D. M. Parragh, C. Scheuerlein, R. Piccin, F. Ravotti, G. Pezzullo, D. Ternova, and M. Taborelli are with CERN, CH1211 Geneva 23, Switzerland (e-mail: Christian.Scheuerlein@cern.ch).

M. Lehner and M. Eisterer are with Atominstitut, Vienna University of Technology, 1020 Vienna, Austria.

Color versions of one or more figures in this article are available at <https://doi.org/10.1109/TASC.2023.3332705>.

Digital Object Identifier 10.1109/TASC.2023.3332705

been characterized by Dynamical Mechanical Analysis (DMA), short beam stress-displacement measurements, impact tests and outgassing measurements.

## II. EXPERIMENTAL

### A. The Samples

In the present study six epoxy resin systems that can be used for the vacuum impregnation of coils for magnets and rotating machines have been characterized before and after irradiation with different sources to dose levels up to 18 MGy.

The CTD101K epoxy system [4], [5] is the baseline impregnation system for the HL-LHC superconducting magnets [6], [7]. This epoxy system consists of diglycidyl ether of bisphenol-A (DGEBA), a carboxylic anhydride hardener, and an accelerator, all of which are supplied by Composite Technology Development Inc. (USA). These components are mixed in the proportion CTD101K resin : hardener : accelerator = 100 parts by weight (pbw) : 90 pbw : 1.5 pbw.

The epoxy resin system MY750 is composed of the Araldite MY750 bisphenol A/epichlorohydrin resin, type DGEBA, average molecular weight MW < 700 (100 pbw) and the aliphatic polyamine hardener Aradur HY5922 (55 pbw) from Huntsman Corporation.

Mix61 also known under the name NHMFL-61 [8], [9], is composed of a diglycidyl ether of bisphenol-A (DGEBA) resin, an aromatic hardener of the amine type, a high molecular weight co-reactant of the amine type and a liquid low molecular weight additive.

The MSUT Twente epoxy system consists of the Araldite MY740 bisphenol A/epichlorohydrin resin (type DGEBA, MW < 700), cured with the carboxylic anhydride hardener of mixed composition Aradur HY906, and the amine accelerator DY062 in the respective ratio 100 pbw : 90 pbw : 0.2 pbw.

More details about the CTD101K, MY750, Mix61 and MSUT processing can be found in [2].

The two-component resin system Huntsman Araldite CY192-1, a cycloaliphatic epoxy resin (100 pbw), and its corresponding anhydride type hardener, Huntsman Aradur HY 918-1 (100 pbw) [10], has been used by CEA Saclay for the impregnation of Nb<sub>3</sub>Sn quadrupole coils [11]. The applied curing cycle recommended by CEA Saclay comprises three isothermal plateaus as follows: 80 °C-24 h, 120 °C-34 h+ 130 °C-12 h.

The epoxy system referred to as Araldite F is used by the company ASG Superconductors S.p.A. for impregnation of magnet coils and consists of the bisphenol A/epichlorohydrin resin (type

DGEBA) Araldite F, the carboxylic anhydride hardener Aradur HY 905, and the polyglycol flexibiliser DY 040. The resin, hardener, and flexibiliser are combined in the ratio of 100 pbw : 100 pbw : 10 pbw, respectively. The Araldite F/Aradur HY 905/flexibiliser DY 040 system does not contain the accelerator DY 061, and filler that is recommended by Huntsman [12].

All samples were cut from 3 mm or 4 mm thick pure epoxy resin plates that were produced by vacuum impregnation at the CERN polymer lab. All samples of a given material were cut from the same plate, thus eliminating uncertainties related to the sample production processes.

### B. Gamma Irradiation

$^{60}\text{Co}$  irradiation has been performed at the Gammatec facility at the Marcoule site of the company Synergy Health Marseille SAS (a Steris company). The irradiations were performed in ambient air at a regulated irradiation temperature of 20–25 °C. Initially identical samples were irradiated to dose levels of 2 MGy, 4 MGy, 6 MGy, 8 MGy and 10 MGy. During irradiation the sample holders were continuously rotated on turntables for better dose homogeneity. Dosimetry measurements were performed with Perspex dosimeters, which were attached at different positions inside and outside the sample holders.

### C. Proton Irradiation

Irradiations with 24 GeV protons have been performed at the CERN IRRAD facility, located in the East Area of the proton synchrotron (PS) accelerator, which is mainly used to qualify particle detector electronics and components for the CERN HEP experiments (trackers and calorimeters) as well as CERN accelerator equipment and material exposed to very high radiation doses. The PS delivers to IRRAD a proton beam of 24 GeV/c, with a typical size of  $12 \times 12 \text{ mm}^2$  in spills of  $\sim 400 \text{ ms}$  duration, every 10 seconds on average. In this beam, samples of  $10 \times 10 \text{ cm}^2$  in size can be exposed typically to a proton fluence of about  $\sim 1.4 \times 10^{16} \text{ p/cm}^2/\text{week}$ . At IRRAD samples can be placed on remotely controlled tables that can be moved transversally and rotate around the beam direction. The shuttle irradiation system can be moved from the outside area to the irradiation position, without the need to stop the proton beam [13].

The dose to a thin object of a given material placed in the proton beam depends primarily on the rate of energy loss of the proton in that material (a thin material has a thickness much smaller than the range of the charged particle in this material). This condition is verified in the case of the irradiated samples (mm-range thickness) irradiated with 24 GeV/c protons (range of several hundred cm in plastic materials). Therefore, the Total Ionizing Dose (TID) in Gy from high-energy protons can be calculated directly from the mass-collision stopping power, assuming  $dE/dx$  for epoxy resins equal to  $1.87 \text{ MeV cm}^2/\text{g}$  and the fluence determined with the activation-foil techniques, as detailed in [14].

### D. Neutron Irradiation

Neutron irradiation was performed in the TRIGA-MARK II reactor in Vienna. The radiation dose results from mixed neutron and gamma radiation. While the latter is easily obtained from the gamma dose rate multiplied by the irradiation time, the energy

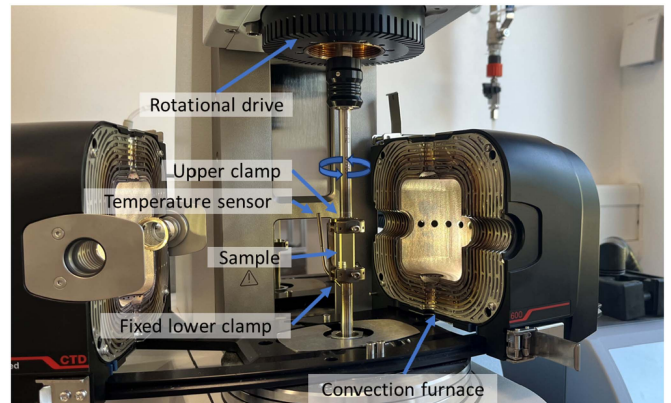


Fig. 1. DMA test configuration.

deposited by the neutrons depends on the elemental composition of the sample and has to be calculated as outlined in [15]. The neutron dose ranges from 1.5 MGy in CDT101K to over 2.1 MGy in MY750 and Mix61 to 2.4 MGy for MSUT at a fast neutron fluence of  $1 \times 10^{21} \text{ m}^{-2}$  ( $E > 0.1 \text{ MeV}$ ). For simplicity the same average value of 2.1 MGy was assumed for all the materials. The simultaneous gamma dose of 4.9 MGy is higher by a factor of more than 2 and independent of the material. The irradiation duration was selected to achieve combined neutron and gamma dose levels of 1 MGy, 3 MGy and 10 MGy.

Before irradiation the samples are sealed in quartz glass capsules to prevent direct contact with the reactor water. Capsules were filled either with ambient air or evacuated to a pressure below  $5 \times 10^{-2} \text{ mbar}$  and then sealed before the start of the irradiation. For outgassing measurements, the samples were irradiated under vacuum.

### E. Dynamic Mechanical Analysis (DMA)

Irradiation induced changes of viscoelastic materials properties were monitored by DMA. The storage modulus ( $G'$ ), which is related to sample stiffness, and the loss modulus ( $G''$ ), which is a measure of the energy dissipated during the applied torsion oscillation, were recorded during temperature sweeps with an Anton Paar Dynamical Mechanical Analyser MCR702e (Fig. 1). The thermal expansion of the sample was estimated from the temperature gap change between the sample fixtures during the temperature sweep.

Measurement of solid bars with dimensions of  $4 \text{ mm} \times 10 \text{ mm} \times 40 \text{ mm}$  was performed according to ASTM D4065, DIN EN ISO 11357, using rectangular fixtures at a frequency of 1 Hz and a temperature ramp of 2 K/min. The glass transition temperature ( $T_g$ ) was determined by three methods, a) the  $G'(T)$  onset according to ISO 11357, b)  $G''(T)$  maximum according to ASTM 4065, and c)  $\tan \delta(T)$  maximum. The  $G'(T)$  transition onset was determined with the Anton Paar Rheo Compass software as the intersection of two tangent lines fitted to  $G'(T)$  [16].

### F. Short Beam Tests

3-point bending short beam tests were performed with a universal test machine using  $\varnothing = 4 \text{ mm}$  loading supports, a  $\varnothing = 10 \text{ mm}$  bending die (Fig. 2), and a constant crosshead speed

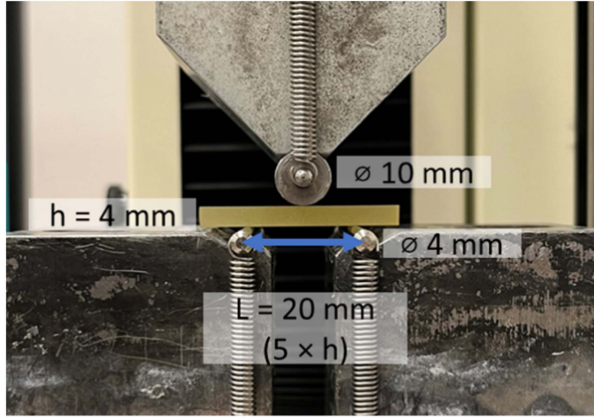


Fig. 2. 3-point bending short beam test configuration.

of 1 mm/min according to ISO 14130:1997 [17]. At least three samples per dose level were tested.

The machine was displacement controlled with a resolution of 0.0001 mm, and force was measured with a resolution of 0.2 N. The samples were rectangular beam specimen with nominal dimensions of 4 mm × 10 mm × 40 mm, and the span length of the loading supports was set as 5 times the average sample thickness per material; on average 20 mm. The short beam stress was calculated according to ISO 14130:1997 as

$$\tau = \frac{3}{4} \cdot \frac{F}{bh}$$

where  $F$  is the load in N, and  $b$  and  $h$  are the width and the thickness of the sample in mm, respectively.

### G. Dynstat Impact Tests

Dynstat impact tests were performed according to DIN 53435 using a pendulum with 2 J nominal impact energy on unnotched rectangular beams with nominal dimensions 4 mm × 10 mm × 15 mm. At least five samples per dose level have been tested.

The impact strength ( $a_{dU}$ ) in kJ/m<sup>2</sup> has been calculated from the energy absorbed by breaking the sample ( $E_c$ ), the sample thickness ( $h$ ) and the sample width ( $b$ ) according to:

$$a_{dU} = \frac{E_c}{bh} \cdot 10^3$$

### H. Fourier Transform Infrared Analysis (FTIR)

Comparative FTIR analysis was conducted on unirradiated and 6 MGy gamma irradiated CTD101K, MY750, and Mix61 resins. Before testing, the samples were ground to reduce surface irregularities and ensure representative bulk analysis for FTIR tests. Spectra were acquired in absorbance mode using a Bruker Vertex 70 spectrometer with ATR accessory (diamond crystal) from 4000 cm<sup>-1</sup> to 400 cm<sup>-1</sup>, employing 32 scans at 4 cm<sup>-1</sup> resolution.

## III. RESULTS

### A. CTD101K Thermomechanical Properties

The  $G'(T)$ ,  $G''(T)$ ,  $\tan \delta(T)$  evolutions and thermal expansion of CTD101K after different gamma ray doses are presented in

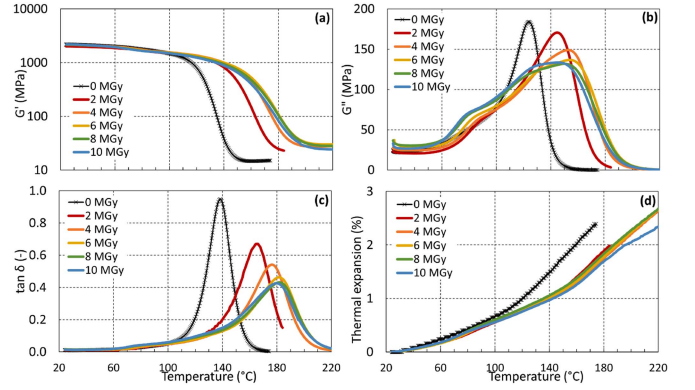


Fig. 3. CTD101K  $G'$ ,  $G''$ ,  $\tan \delta$ , and thermal expansion as a function of temperature measured before and after gamma irradiation up to 10 MGy.

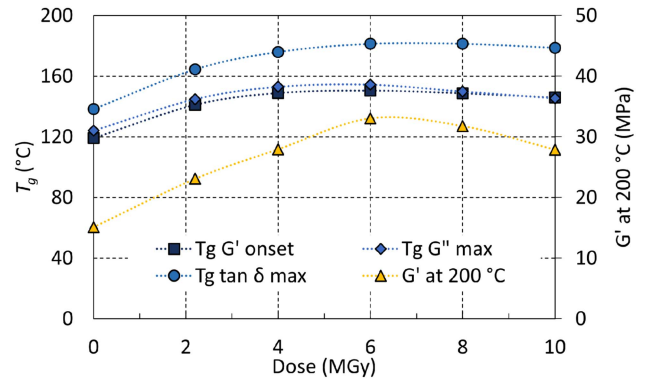


Fig. 4. CTD101K glass transition temperature  $T_g$ ,  $G'$  onset,  $T_g$   $G''$  max, and  $T_g$   $\tan \delta$  max, and rubbery storage modulus  $G'$  at 200 °C as a function of absorbed gamma irradiation dose. The dashed lines are a guide to the eye.

Fig. 3. Initially the glass transition temperature of the CTD101K system increases with irradiation dose, presumably because of formation of new cross-links. An increase in cross-link density is also indicated by an increase of the storage modulus in the rubbery regime above the glass transition temperature.

The change of slopes of thermal expansion curves (Fig. 3 (d)) is a further indication that the glass transition temperature is exceeded. The  $G''$  and  $\tan \delta$  peak widths (FWHM) increase with increasing dose, indicating that the  $T_g$  spread within the sample increases with increasing dose.

In Fig. 4 the  $T_g$  values determined from  $G'(T)$ ,  $G''(T)$  and  $\tan \delta$  max are plotted as a function of the absorbed gamma dose. The highest  $T_g$  is obtained after an absorbed dose of 6 MGy ( $G''$  max is increased by 30 °C from 124 °C to 154 °C). Further increasing the irradiation dose reduces the glass transition temperature.

Similarly, the rubbery like shear modulus measured above  $T_g$  increases with increasing irradiation dose from 15 MPa before irradiation to a maximum value of 33 MPa after 6 MGy absorbed dose. Further increasing the dose to 10 MGy reduces  $G'$  at 200 °C to 28 MPa.

In Fig. 5 the  $T_g$  vs irradiation dose evolution of CTD101K is compared for gamma irradiation and proton irradiation at ambient temperature. A similar trend is observed, with a maximum  $T_g$  after an absorbed dose of about 6 MGy.

In addition to the DMA measurements, 3-point bending tests were also performed on the gamma irradiated samples. As seen

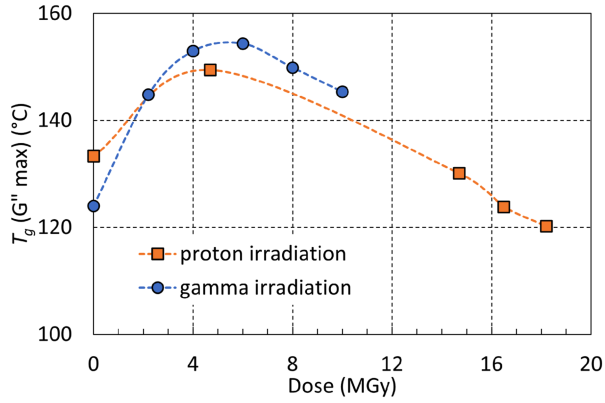


Fig. 5.  $T_g$  evolution of CTD101K as a function of gamma and proton irradiation dose in ambient air. The dashed lines are a guide to the eye.

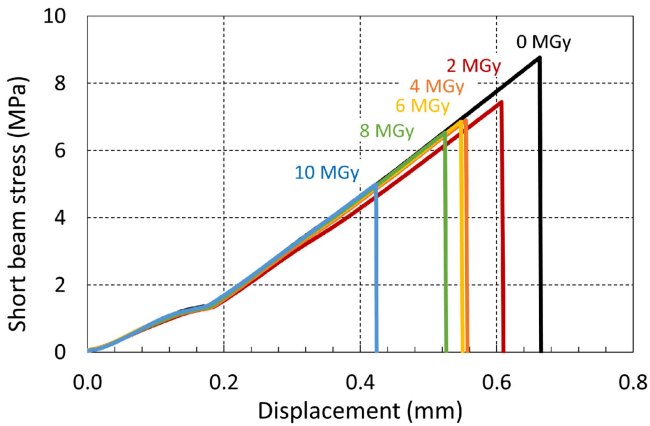


Fig. 6. Short beam stress-displacement curves of pure CTD101K before and after gamma irradiation in ambient air up to 10 MGy.

from the linear slope of the short beam stress-displacement curves of Fig. 6, the ambient temperature modulus of the CTD101K epoxy system is not significantly changed after the irradiation up to 10 MGy, despite the increased cross-link density revealed by an increased  $T_g$  and  $G'$  at 200 °C. The strain at fracture is reduced with increasing dose, indicating that irradiation makes the CTD101K resin more brittle.

### B. Mix61 Thermomechanical Properties

The  $G'(T)$ ,  $G''(T)$ ,  $\tan \delta(T)$  and thermal expansion evolutions of Mix61 after different gamma ray doses are presented in Fig. 7. After a dose of 10 MGy,  $T_g$  as determined from  $\tan \delta$  maximum is decreased by 13 °C. The glass transition onset of Mix61 is below room temperature (RT) and is not revealed by the present DMA temperature sweeps.

The ambient temperature storage modulus initially increases from 770 MPa (0 MGy) to 920 MPa (2 MGy), and then decreases at higher irradiation doses. The rubbery like shear modulus measured above  $T_g$  at 90 °C decreases with increasing irradiation dose from 10.3 MPa before irradiation to 0.8 MPa after 10 MGy, indicating that chain scission is the dominating process.

The short beam stress-displacement curves of Mix61 after different gamma irradiation doses are presented in Fig. 8. After 2 MGy gamma irradiation the modulus and short beam strength

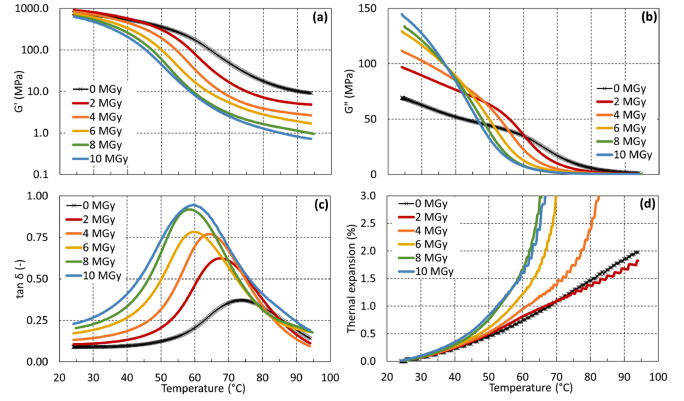


Fig. 7. Mix 61  $G'$ ,  $G''$ ,  $\tan \delta$ , and thermal expansion as a function of temperature measured before and after gamma irradiation up to 10 MGy.

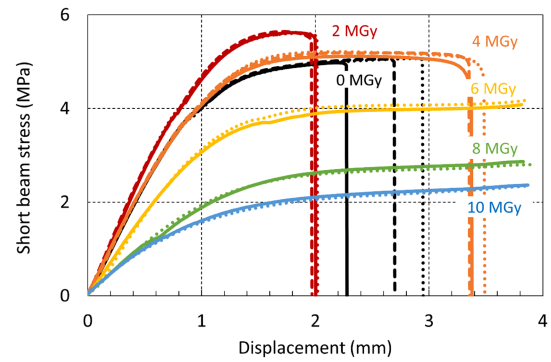


Fig. 8. Short beam stress-displacement curves of Mix61 before and after gamma irradiation in ambient air to different doses.

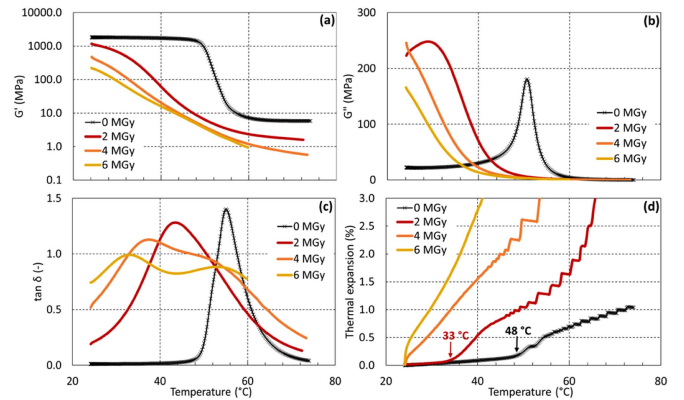


Fig. 9. MY750  $G'$ ,  $G''$ ,  $\tan \delta$ , and thermal expansion as a function of temperature measured before and after gamma irradiation up to 6 MGy.

are increased with respect to the unirradiated sample. Higher doses decrease the modulus, which is consistent with the storage modulus results of Fig. 8. With further increasing dose the short beam strength is reduced and the strain at rupture is increased.

### C. MY750 Thermomechanical Properties

The  $G'(T)$ ,  $G''(T)$ ,  $\tan \delta(T)$  and thermal expansion evolutions of MY750 after different gamma ray doses are presented in Fig. 9, and the corresponding MY750 short beam stress-displacements curves are presented in Fig. 10.

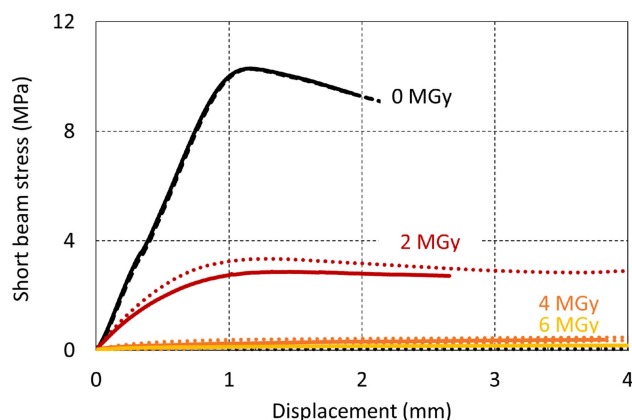


Fig. 10. Short beam stress-displacement curves of MY750 before and after gamma irradiation in ambient air to different doses.

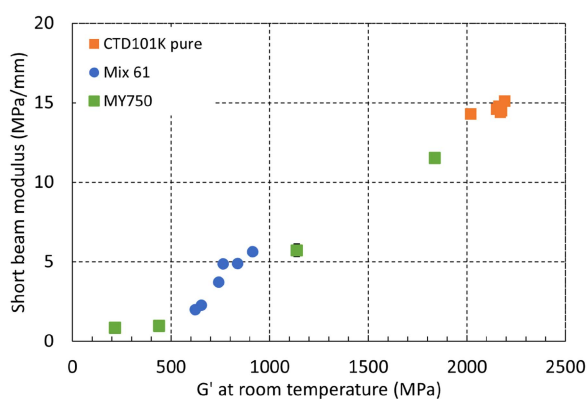


Fig. 11. Short beam modulus at RT as a function of  $G'$  at RT of CTD101K, Mix61, and MY750.

As shown in Fig. 10, already after 2 MGy the MY750 stiffness and strength are strongly reduced. After 4 MGy the MY750 glass transition temperature is below RT, the mechanical strength is drastically reduced, and the sample is so ductile that it cannot be fractured in the 3-point bending test configuration.

#### D. Comparison of DMA and Short Beam Results

In Fig. 11, the short beam moduli of the unirradiated and gamma irradiated CTD101K, Mix61 and MY750 samples are plotted as a function of the corresponding storage moduli determined at the same temperature. The RT short beam moduli and storage moduli are correlated, as expected, for the isotropic pure polymers studied here.

#### E. Comparison of Impact and Short Beam Results

The CTD101K, MY750 and Mix61 RT impact strength as a function of the absorbed dose is presented in Fig. 12. The unirradiated Mix61 and MY750 exhibit comparatively higher impact strength than CTD101K, but after an absorbed dose of 2 MGy the Mix61 and MY750 impact strength is already drastically reduced below that of CTD101K.

The work to fracture of the static short beam test (area under the stress-displacement curves) is correlated with the dynamic impact strength. The work of fracture and impact strength evolution of Mix61 exhibits an unusual behavior, where at

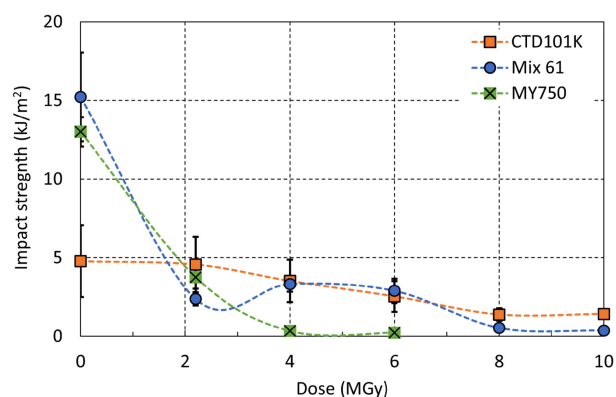


Fig. 12. Dynstat impact strength of CTD101K, Mix61, and MY750 as a function of the absorbed dose. The dashed lines are a guide to the eye.

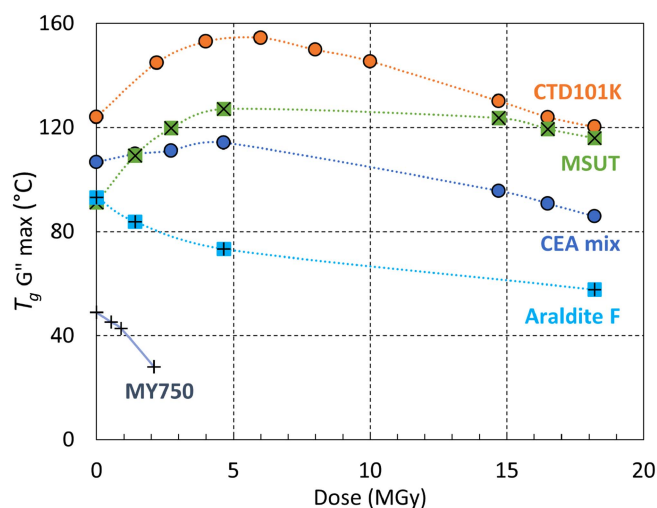


Fig. 13. Evolution of the glass transition temperature  $T_g$  ( $G''$  max) of different epoxy resins as a function of the absorbed dose (gamma or 24 GeV proton irradiation). The dashed lines are a guide to the eye.

4 MGy and 6 MGy both are increased with respect to the 2 MGy values.

#### F. Comparison of Aging Rates Based on $T_g$ Evolution

In Fig. 13 the evolution of the glass transition temperature of five epoxy resin systems as a function of the absorbed dose is plotted.

The CTD101K and CEA mix resin  $T_g$  vs dose evolution is similar, with a first increase of  $T_g$  up to about 6 MGy, presumably because the cross-linking yield exceeds the chain scission yield. At higher doses  $T_g$  decreases with dose, indicating that the chain scission prevails. Above 15 MGy,  $T_g$  of both resins decreases with a rate of about minus 3 °C/MGy. Assuming that this rate remains constant also at higher doses, it is estimated that the glass transition of the CTD101K system falls below ambient temperature after a dose of roughly 50 MGy.

For MSUT the  $T_g$  evolution up to 18 MGy might suggest that this epoxy system has comparatively higher irradiation tolerance. Irradiation of MSUT is ongoing to assess the irradiation induced ageing rate at higher doses.

For the Araldite F and MY750 epoxy resin systems  $T_g$  decreases with increasing dose already at very low doses. The

irradiation induced aging of MY750 is comparatively fast. Initially the MY750  $T_g$  ( $G''$  max) decreases with a rate of minus  $9.2\text{ }^\circ\text{C}$  per MGy. Already after an absorbed dose of less than 3 MGy, the  $T_g$  of MY750 is below RT.

The glass transition onset of the unirradiated Mix61 system is below RT, and therefore the  $G''$  max evolution of Mix61 was not determined in the present study. The  $\tan \delta$  max results suggest that after 10 MGy absorbed dose the Mix61 glass transition temperature is reduced by about  $20\text{ }^\circ\text{C}$ .

### G. Neutron Irradiation Induced Outgassing

The irradiation induced outgassing was measured after 10 MGy combined neutron and gamma irradiation under vacuum. The volume of generated gas was determined from the pressure after breaking the capsules in an evacuated container of known volume, by assuming the pressure-volume relation of an ideal gas. Each irradiated sample has a volume of  $1.6\text{ cm}^3$ .

The CTD101K ( $3.2 \pm 0.1\text{ cm}^3/\text{g}$ ) and MSUT ( $4.0 \pm 0.2\text{ cm}^3/\text{g}$ ) epoxy resins exhibit about three times less outgassing as compared to the MY750 ( $12 \pm 0.3\text{ cm}^3/\text{g}$ ) and Mix61 ( $10 \pm 0.1\text{ cm}^3/\text{g}$ ) epoxy resins.

After 10 MGy neutron irradiation, bubbles have formed in the Mix61 and MY750 samples. The additional gas content in these bubbles was not detected by the outgassing measurements. The CTD101K and MSUT samples did not show any bubble formation.

### H. FTIR Analysis

After an absorbed dose of 6 MGy, the spectra of the two amino-cured resins MY750 and Mix61 exhibited similar changes observed at the following spectral positions: a reduction in the broad OH band around  $3400\text{ cm}^{-1}$ , possibly due to hydrogen bond formation with some newly created functional groups as a consequence of irradiation; emergence of a broad band around  $3250\text{ cm}^{-1}$ , potentially indicating amine group formation or hydrogen bonding of existing OH groups; the appearance of shoulders around the  $1600\text{ cm}^{-1}$  peak, suggesting the generation of C=C bonds in the amine links or backbone. Overall, the radiation-induced alterations in Mix61 seemed less pronounced than those in MY 750, likely due to the presence of an aromatic hardener in the latter, known to be less susceptible to irradiation [18].

The anhydride-cured CTD101K resin exhibited the most marked radiation-induced spectral changes. After 6 MGy absorbed dose, where  $T_g$  reached its maximum value, virtually all peaks, particularly in the fingerprint region, revealed substantial alterations in the resin structure. Interestingly, the spectrum of unirradiated CTD101K resin showed peaks at  $913\text{ cm}^{-1}$  corresponding to unreacted oxirane groups and  $1780\text{ cm}^{-1}$  for anhydride groups. These peaks disappeared after irradiation, suggesting a radiation-induced post-curing effect. This aligns with existing literature on radiation-curable epoxy resins [19] and it is consistent with the CTD101K  $T_g$  and  $G''(200\text{ }^\circ\text{C})$  evolutions shown in Fig. 4.

## IV. DISCUSSION AND CONCLUSION

In the frame of the CERN polymer lab irradiation study of polymers for possible application in future superconducting accelerator magnets, the effect of gamma, proton and neutron

irradiation on the thermomechanical properties, the visual aspect, and outgassing of different epoxy resin systems has been assessed.

Unlike most previous irradiation studies, in the present study we have irradiated pure resins without fibre reinforcement, where mechanical tests can directly reveal the epoxy resin aging. Mechanical tests of the strongly anisotropic fibre reinforced samples are dominated by the fibre volume fraction, fibre orientation, fibre material and sizing, and they are much less sensitive to irradiation induced changes of the resin matrix, in particular when mechanical stresses are applied in the fibre direction.

DMA measurements require only a comparatively small sample volume, which is highly advantageous for irradiation studies where only small volumes can be irradiated and where samples are activated, and aging rates of the different polymers when irradiated with different sources and in different environments can be compared. The competing irradiation induced processes cross-linking and chain scission are revealed by changes of  $T_g$  as a function of the absorbed dose.

The DMA results suggest that the aging of the CTD101K, CEA mix and MSUT epoxy resin systems occurs with a comparatively low rate. For CTD101K and CEA mix a  $T_g$  maximum is achieved after about 6 MGy, the MSUT aging rate appears to be particularly low. This will be verified by tests after ongoing irradiations up to 30 MGy.

The MY750 and Mix61 epoxy resin systems with amine-based hardeners exhibit relatively high irradiation induced outgassing. MY750 is the fastest aging of the epoxy resins studied. Already after an absorbed dose of 2 MGy its mechanical strength is drastically reduced. The MY750  $T_g$  is reduced with a comparatively high rate of about minus  $9\text{ }^\circ\text{C}/\text{MGy}$ , and after 4 MGy dose MY750 is at RT in the rubbery state and cannot transmit substantial mechanical loads. This may suggest that amine-based hardeners should be avoided for epoxy systems that are exposed to high radiation doses [20].

For the epoxy systems studied so far, the same absorbed dose of proton and gamma irradiation has a similar effect. The effect of neutron irradiation in research reactors and spallation sources on the thermomechanical epoxy resin properties is being studied.

The results presented here are a first step of the irradiation study that aims to predict the changes of the functional polymer properties under the irradiation fields and the irradiation environment in superconducting magnets, at cryogenic temperature in the absence of oxygen. Therefore, the RT irradiation results presented here can be considered as pessimistic, and it is likely that aging in liquid helium atmosphere will occur at lower rates. Irradiations of epoxy resins in liquid helium and in inert gas at ambient temperature have been performed at the CERN IRRAD facility and characterizations of these irradiated samples are ongoing.

In addition to the pure resin irradiation studies presented here, the irradiation induced aging of fibre reinforced composites is being studied for selected insulation systems.

## ACKNOWLEDGMENT

We would like to thank Davide Tommasini for his support and advice. We are grateful to the Steris team for the gamma irradiations and dosimetry at the Gammatec facility.

## REFERENCES

- [1] A. Abada et al., "FCC-hh: The Hadron Collider," *Eur. Phys. J. Special Topics*, vol. 228, no. 4, pp. 755–1107, 2019.
- [2] A. Brem, B. J. Gold, B. Auchmann, D. Tommasini, and T. A. Tervoort, "Elasticity, plasticity and fracture toughness at ambient and cryogenic temperatures of epoxy systems used for the impregnation of high-field superconducting magnets," *Cryogenics*, vol. 115, 2021, Art. no. 103260.
- [3] P. Ebermann et al., "Irreversible degradation of Nb<sub>3</sub>Sn Rutherford cables due to transversal compression stress at room temperature," *Supercond. Sci. Technol.*, vol. 31, 2018, Art. no. 065009.
- [4] P. E. Fabian, N. A. Munshi, and R. J. Denis, "Highly radiation-resistant vacuum impregnation resin systems for fusion magnet insulation," in *Proc. AIP Conf.*, 2002, vol. 614, pp. 295–304.
- [5] A. Gaarud, D. M. Parragh, S. Clement, C. Scheuerlein, R. Piccin, and R. Lach, "Improved fracture toughness at cryogenic temperature of irradiation hard epoxy system for superconducting coil impregnation," submitted for publication, [Online]. Available: <http://ssrn.com/abstract=4478135>
- [6] L. Bottura, G. de Rijk, L. Rossi, and E. Tedesco, "Advanced accelerator magnets for upgrading the LHC," *IEEE Trans. Appl. Supercond.*, vol. 25, no. 3, Jun. 2015, Art. no. 4002107.
- [7] E. Todesco et al., "The high luminosity LHC interaction region magnets towards series production," *Supercond. Sci. Technol.*, vol. 34, 2021, Art. no. 053001.
- [8] A. B. Brennan, T. M. Miller, J. J. Arnold, K. V. Huang, N. L. Gephart, and W. D. Markewicz, "Thermomechanical properties of a toughened epoxy for impregnation superconducting magnets," *Cryogenics*, vol. 35, no. 11, pp. 783–785, 1995.
- [9] W. D. Markewicz, I. R. Dixon, J. L. Dougherty, K. W. Pickard, and A. B. Brennan, "Properties of epoxy NHMFL 61 for superconducting magnet impregnation," presented at the ICMC/CEC 1997, Portland, OR, USA, 1997.
- [10] Huntsman Araldite impregnation resin system Araldite CY192-1 100 pbw Aradur HY 918-1 100 pbw data sheet.
- [11] J. M. Rifflet, M. Durante, and M. Segreti, "Nb<sub>3</sub>Sn quadrupole development at CEA Saclay," in *Proc. Wamsdo 2008*, E. Todesco, Ed., CERN, Geneva, Switzerland, 2009. [Online]. Available: <https://cdsweb.cern.ch/record/1162820/files/cern-2009-001.pdf>
- [12] "Araldite casting resin system," Huntsman data sheet, May 2004. [Online]. Available: <https://www.gluespec.com/Materials/SpecSheet/484420d9-3d7b-479d-a0cd-4c3204a86877>
- [13] F. Ravotti, B. Gkotse, M. Glaser, P. Lima, E. Matli, and M. Moll, "A new high-intensity proton irradiation facility at the CERN PS east area," in *Proc. Int. Conf. Technol. Instrum. Part. Phys.*, 2014, pp. 354–358. [Online]. Available: <https://pos.sissa.it/213/354/pdf>, doi: [10.22323/1.213.0354](https://doi.org/10.22323/1.213.0354).
- [14] F. Ravotti, "Dosimetry techniques and radiation test facilities for total ionizing dose testing," *IEEE Trans. Nucl. Sci.*, vol. 65, no. 8, pp. 1440–1464, Aug. 2018, doi: [10.1109/TNS.2018.2829864](https://doi.org/10.1109/TNS.2018.2829864).
- [15] H. W. Weber, "Radiation effects on superconducting fusion magnet components," *Int. J. Modern Phys. E*, vol. 20, no. 6, 2011, pp. 1325–1378.
- [16] *Standard Test Method for Glass Transition Temperature (DMA Tg) of Polymer Matrix Composites by Dynamic Mechanical Analysis (DMA)*, Standard D7028-07, ASTM, West Conshohocken, PA, USA, 2015.
- [17] *Fibre-Reinforced Plastic Composites Determination of Apparent Interlaminar Shear Strength by Short-Beam Method*, Standard 14130:1997, ISO, Geneva, Switzerland, 1997.
- [18] Y. Ngono and Y. Maréchal, "Epoxy-amine reticulates observed by infrared spectrometry. II. Modifications of structure and of hydration abilities after irradiation in a dry atmosphere," *J. Polym. Sci.: Part B: Polym. Phys.*, vol. 38, pp. 329–340, 2000.
- [19] G. Spadaro, E. Calderaro, E. Tomarchio, and C. Dispenza, "Novel epoxy formulations for high energy radiation curable composites," *Radiat. Phys. Chem.*, vol. 72, pp. 465–473, 2005.
- [20] S. Tagawa, M. Washio, N. Hayashi, and Y. Tabata, "Pulse radiolysis studies on radiation resistance of epoxy resin," *J. Nucl. Mater.*, vol. 133/134, pp. 785–787, 1985.